ELSEVIER

Journal of Organometallic Chemistry 488 (1995) 199–204

Journal of Organometallic Chemistry

Octahedral iridium carbonyl clusters. Synthesis, characterization and solid state structure of the nitrosyl cluster $[Ir_6(CO)_{11}(\mu\text{-}CO)_3NO]^-$ ☆

Roberto Della Pergola *[a], Luigi Garlaschelli [a], Mario Manassero [b], Norberto Masciocchi *[b]

[a] *Dipartimento di Chimica Inorganica, Metallorganica ed Analitica, via G. Venezian 21, 20133 Milano, Italy*
[b] *Istituto di Chimica Strutturistica Inorganica, via G. Venezian 21, 20133 Milano, Italy*

Received 1 August 1994

Abstract

The nitrosylcarbonyl cluster $[Ir_6(CO)_{14}NO]^-$ has been prepared by one-electron oxidation of $[Ir_6(CO)_{15}]^{2-}$, followed by addition of NO at low temperature. The structure of the salt $[NMe_3(CH_2Ph)][Ir_6(CO)_{11}(\mu\text{-}CO)_3NO]$ was solved by direct methods and difference Fourier techniques and refined down to $R = 0.036$, for 3239 observed reflections having $I > 3\sigma(I)$. The cluster of idealized C_s point group symmetry contains an octahedral metal framework of iridium atoms, an NO group linearly bound, which acts as a three-electron donor, 11 terminal and three edge-bridging carbonyl ligands. The Ir–N separation of 1.75(3) Å is the shortest metal-to-ligand bond distance. Average distances are: Ir–Ir = 2.773 Å, $Ir\text{–}C_{term}$ = 1.86 Å, $C_{term}\text{–}O_{term}$ = 1.16 Å, $Ir\text{–}C_{bridg}$ = 2.02 Å, $C_{bridg}\text{–}O_{bridg}$ = 1.19 Å.

Keywords: Iridium; Carbonyls; Cluster; Nitrosyl; Crystal structure; Octahedron

1. Introduction

In recent years, we have devised a simple method for the synthesis of monosubstituted hexanuclear iridium carbonyl clusters, based upon the electrochemical evidence for the reactive species $[Ir_6(CO)_{15}]^{n-}$ ($n = 0$ or 1) [1]. These labile complexes can add rapidly a large variety of electron donor fragments, yielding substituted derivatives. This approach represents a very useful alternative to the nucleophilic attack on the neutral $[Ir_6(CO)_{16}]$ and allows the addition of halides, pseudohalides, substituted alkynes, or diorganophosphines [2–4]. In order to check the generality of this method, we tried to obtain a nitrosyl-substituted carbonyl cluster which had already reported and was supposed to have a bent NO. On the basis of its IR spectrum it was formulated as $[Ir_6(CO)_{15}NO]^-$ [5]. The IR data of the compound obtained by us did not correspond exactly to those already reported, and this prompted further investigation and, eventually, a full structural determination, which revealed a different formulation and a linear coordination for the nitrosyl group.

2. Results

2.1. Synthesis of $[Ir_6(CO)_{14}NO]^-$

The one-electron oxidation of $[Ir_6(CO)_{16}]^{2-}$ in tetrahydrofuran (THF) can be accomplished smoothly with ferrocenium or tropylium cations, yielding the radical monoanion which can be easily detected by IR (ν_{CO} at 2021vs, 1821m cm^{-1}) or ESR spectroscopy [1]. It is stable for several hours, even at room temperature, but it decomposes to species of higher nuclearity on standing in solution for longer periods.

Bubbling of NO into the solution resulted in an immediate colour change of the solution, and slight modification of the IR spectrum. A very large excess of NO, or direct addition to $[Ir_6(CO)_{15}]^{2-}$, brought about the formation of uncharacterized, insoluble species. The best results were obtained when the gas was carefully added at −78°C. The FT-IR spectrum recorded immediately after the addition of NO showed a large number of bands, suggesting the presence of cluster compounds different from the starting material

---

☆ Dedicated to Prof. Fausto Calderazzo for his outstanding contribution to inorganic chemistry.

* Corresponding authors.

SSDI 0022-328X(94)00022-0

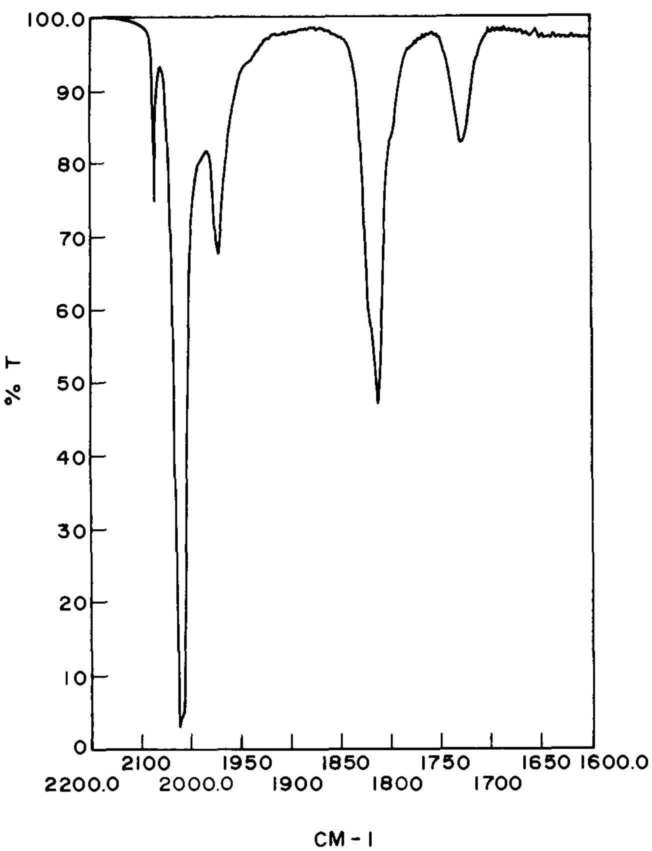

Fig. 1. The IR spectrum of $[N(PPh_3)_2][Ir_6(CO)_{14}NO]$ in THF.

and product. Computer subtraction of the spectra showed two absorptions at 2042 cm^{-1} and 1793 cm^{-1}, confidently assigned to the unstable intermediate $[Ir_6(CO)_{15}NO]^-$.

The reaction mixture was then warmed up to room temperature and the IR spectrum showed the presence of a single compound which was thoroughly characterized as $[Ir_6(CO)_{14}NO]^-$. The complete scheme of the reaction can be represented by Eqs. 1–3.

$$[Ir_6(CO)_{15}]^{2-} + [C_7H_7]^+ \rightarrow [Ir_6(CO)_{15}]^- + 1/2[C_7H_7]_2 \quad (1)$$

$$[Ir_6(CO)_{15}]^- + NO \rightarrow [Ir_6(CO)_{15}NO]^- \quad (2)$$

$$[Ir_6(CO)_{15}NO]^- \rightarrow [Ir_6(CO)_{14}NO]^- + CO \quad (3)$$

Selected crystals of $[N(PPh_3)_2][Ir_6(CO)_{14}NO]$ show IR absorption bands in THF at 2069mw, 2023vs, 1971mw, 1812m, 1727w cm^{-1} (Fig. 1). The shape of the spectrum is very similar to that of the octahedral clusters $[Ir_6(CO)_{12}(\mu\text{-}CO)_2(\mu\text{-}X)]^-$ (X = Cl, Br, I, SCN, or PPh_2), [2–4] and the absorption at 1727 cm^{-1} suggest the presence of a terminal, linear, NO [6].

Stevens et al. [5] reported that the nucleophilic addition of $[N(PPh_3)_2]NO_2$ to $[Ir_6(CO)_{16}]$ leads to $[Ir_6(CO)_{15}NO]^-$, according to Eq. 4.

$$[Ir_6(CO)_{16}] + [N(PPh_3)_2]NO_2 \rightarrow [N(PPh_3)_2][Ir_6(CO)_{15}NO] + CO_2 \quad (4)$$

However, an excess of nitrite caused further reduction to $[Ir_6(CO)_{15}]^{2-}$, and caused unavoidable impurity of the product. A very weak absorption was detected at 1457 cm^{-1}, and assigned to a bent NO (a one-electron donor): the cluster was formulated $[Ir_6(CO)_{15}NO]^-$ [5]. As all the other IR bands (except that at 1727 cm^{-1}) are very similar to those recorded by us and because we have evidence that $[Ir_6(CO)_{15}NO]^-$ is very unstable, we think the two products are the same material.

However, the preparation reported here has definite advantages over that in Eq. (4), because it avoids the intermediate isolation of the neutral $[Ir_6(CO)_{16}]$ and allows a product of higher purity, as shown by the excellent elemental analysis.This preparation does not require any specific cation, so that several different salts could be synthesized, crystallized and analyzed by X-ray analysis. Conversely, the reaction of Eq. (4) is made possible by the unique solubility and stability properties of $[N(PPh_3)_2]NO_2$ [7,8] although the crystals of $[N(PPh_3)_2][Ir_6(CO)_{14}NO]$ that resulted were unsuitable for solid-state structure determination (see below).

2.2. Solid-state structure of $[NMe_3(CH_2Ph)][Ir_6(CO)_{11}(\mu\text{-}CO)_3NO]$

The crystals of $[NMe_3(CH_2Ph)][Ir_6(CO)_{14}NO]$ consist of discrete tetrasubstituted ammonium cations and

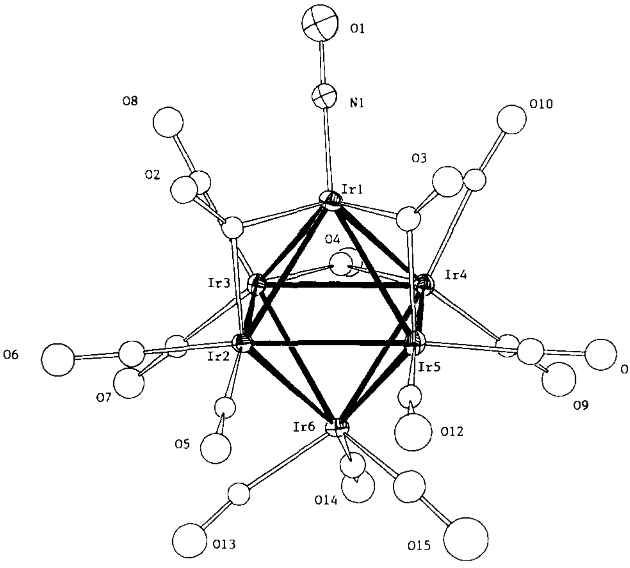

Fig. 2. ORTEP drawing of $[Ir_6(CO)_{14}NO]^-$. Carbonyl carbon atoms are labelled as the oxygen atoms to which they are attached. Thermal ellipsoids are drawn at 30% probability.

Table 1
Selected bond distances (Å) and angles (deg.) for $[NMe_3(CH_2Ph)]$-$[Ir_6(CO)_{14}(NO)]$

Ir1–Ir2 2.743(2)	Ir2–Ir6 2.808(2)	⟨Ir–Ir⟩ 2.773
Ir1–Ir3 2.786(2)	Ir3–Ir4 2.719(3)	⟨Ir–Ir⟩ 2.743 bridged
Ir1–Ir4 2.792(2)	Ir3–Ir6 2.760(2)	⟨Ir–Ir⟩ 2.783 unbridged
Ir1–Ir5 2.741(3)	Ir4–Ir5 2.764(2)	min. 2.719(3)
Ir2–Ir3 2.771(2)	Ir4–Ir6 2.766(2)	max. 2.808(2)
Ir2–Ir5 2.796(3)	Ir5–Ir6 2.807(3)	
Ir–N1 1.75(3)	N1–O1 1.20(4)	Ir1–N1–O1 178(3)
Ir1–C2 1.97(3)	C2–O2 1.20(3)	Ir1–C2–O2 141(3)
Ir1–C3 1.98(3)	C3–O3 1.15(4)	Ir1–C3–O3 139(2)
Ir2–C2 2.02(3)		Ir2–C2–O2 134(2)
Ir2–C5 1.86(3)	C5–O5 1.16(3)	Ir2–C5–O5 179(3)
Ir2–C6 1.88(3)	C6–O6 1.21(4)	Ir2–C6–O6 176(3)
Ir3–C4 1.97(3)	C4–O4 1.22(4)	Ir3–C4–O4 137(3)
Ir3–C7 1.86(3)	C7–O7 1.14(4)	Ir3–C7–O7 179(3)
Ir3–C8 1.88(3)	C8–O8 1.13(4)	Ir3–C8–O8 176(3)
Ir4–C4 2.02(3)		Ir4–C4–O4 134(3)
Ir4–C9 1.87(3)	C9–O9 1.16(4)	Ir4–C9–O9 173(3)
Ir4–C10 1.89(3)	C10–O10 1.15(4)	Ir4–C10–O10 175(3)
Ir5–C3 2.18(3)		Ir5–C3–O3 135(3)
Ir5–C11 1.89(4)	C11–O11 1.15(4)	Ir5–C11–O11 177(4)
Ir5–C12 1.85(3)	C12–O12 1.24(4)	Ir5–C12–O12 176(3)
Ir6–C13 1.90(5)	C13–O13 1.11(4)	Ir6–C13–O13 169(3)
Ir6–C14 1.82(4)	C14–O14 1.18(4)	Ir6–C14–O14 174(3)
Ir6–C15 1.79(5)	C15–O15 1.25(6)	Ir6–C15–O15 158(4)
Average values		
Terminal COs		
⟨Ir–C⟩ 1.86	⟨C–O⟩ 1.16	⟨Ir–C–O⟩ 174
Bridging COs		
⟨Ir–C⟩ 2.02	⟨C–O⟩ 1.19	⟨Ir–C–O⟩ 137

$[Ir_6(CO)_{14}NO]^-$ anions, with no short interionic contacts. An ORTEP view [9] of the whole anion with atomic labelling scheme is shown in Fig. 2; selected bond distances and angles are supplied in Table 1. $[Ir_6(CO)_{14}NO]^-$ contains an octahedral metallic framework surrounded by 12 terminal and three edge-bridging ligands.

The size and the bonding properties of linear nitrosyl and CO ligands are very similar. X-ray methods can distinguish between carbonyl and nitrosyl [6] upon the refinement of the thermal factors of the ligand atoms. However, in high nuclearity clusters the presence of heavy elements or disordered structures can prevent the correct assignment of the nitrogen atom(s) [10]. Nevertheless, when the metal atoms are differently connected, it is possible to predict the location of the nitrosyl group(s) with the aid of chemical considerations and spectroscopic (IR and NMR) data. In such cases [11–13], metal–nitrogen and N–O bond distances have been confidently assessed and show that NO groups typically possess metal–nitrogen distances about 0.05 Å shorter than the metal–carbon values.

The location of the nitrogen atom (and the consequent labelling of the nitrosyl group) in $[Ir_6(CO)_{14}NO]^-$ could only be identified by a combination of spectroscopic and structural observations. The IR data are consistent with a terminal nitrosyl group. The carbonyl stereochemistry shows that each metal vertex is connected to three ligands [Ir(6) is bound to three terminal groups; Ir(1) bears two bridging and one terminal ligands; the four remaining iridium atoms are linked to two terminal and one edge-bridging CO, as commonly found in many iridium octahedral clusters]. Thus, Ir(6) is electron rich and Ir(1) is electron deficient. The terminal group bound to the latter should therefore be NO, and considered to be a three-electron donor.

The anion possesses C_s idealized symmetry, with the mirror plane passing through the Ir(1), Ir(6) and the NO group. Deformations of the metal framework conform to this pattern, so that corresponding Ir–Ir bond distances differ by less than 0.01 Å [min. 2.719(3) Å, max. 2.808(2) Å, average 2.773 Å, $Q = 1.9$ [14]]. The CO-spanned Ir–Ir distances are slightly shortened by the bridging carbonyls. The average values for bridged and unbridged metal–metal interactions are 2.743 Å and 2.783 Å, respectively as repeatedly observed in clusters with six or more iridium atoms, though the opposite occurs for tetrahedral species [15,16].

Bridging carbon–oxygen distances (average 1.19 Å) are lengthened by increased π back-donation, in comparison with terminal carbonyl groups (average 1.16 Å). Two terminal carbonyls on Ir(6) are bent towards Ir(2) and Ir(5) [158(4)° and 169(3)°, respectively], dissipating the high electron density formally present on those metal atoms, while all the other terminal carbonyls are almost linear [average to 176°].

Further support to the assignment of the nitrosyl

Table 2
Summary of data for different crystalline salts of $[Ir_6(CO)_{14}(NO)]^-$

Cation	$[NEt_4]^+$	$[N(PPh_3)_2]^+$	$[PPh_4]^+$	$[NMe_3(CH_2Ph)]^+$
Crystal system	orthorhombic	monoclinic	orthorhombic	trigonal
Space group	$C222_1$	$P2_1/a$	$P2_12_12_1$	$P3_1$
a, Å	11.933(1)	22.289(4)	15.400(2)	12.150(4)
b, Å	14.619(2)	13.359(4)	16.991(2)	
c, Å	18.874(5)	28.840(4)	20.833(3)	19.598(18)
β, deg.		116.02(1)		
Color	black	brown	black	black
Shape	lamellae	lamellae	needles	needles
R	0.043	0.037	0.086	0.036
Comment	disordered metals 60:40	disordered COs, C_{2v}	fast decay 2 indep. molec	ordered NO

ligand derives from the refined value of its Ir–N bond distance [1.75(3) Å] which is by far the shortest metal-to-ligand interaction, present in this compound. Although a bond distance of 1.79(5) Å was found for the Ir(6)–C(15) interaction, this second shortest bond length cannot be attributed to a terminal NO group, for it is attached to the electron-rich Ir(6) atom.

Metal–nitrogen bond lengths observed in the few structurally characterized penta- and hexa-nuclear carbonyl clusters containing terminal NO groups (1.78(1) Å in $[Ru_6C(CO)_{14}(NO)_2]$ [12], 1.72(1) Å in $[Ru_6C(CO)_{15}(NO)(AuPPh_3)]$ [12], 1.76(2) Å in $[Ru_5C(CO)_{13}(NO)(\mu_2\text{-}AuPEt_3)]$ and 1.81(2) Å in $[Ru_5C(CO)_{13}(NO)(\mu_3\text{-}AuPEt_3)]$ [13]) are consistent with the value found in $[Ir_6(CO)_{14}NO]^-$.

Several structural determinations of $[Ir_6(CO)_{14}NO]^-$ crystallized with different cations have been performed, Table 2, and have shown varying degrees of disorder. Two points are worthy of note. First, if the two asymmetric carbonyls on Ir(6) are moved into truly bridging position and the two μ_2-CO's on Ir(1) become bent terminal groups, the geometry of the ligands around the Ir(1) and Ir(16) vertex are switched. Such small reorganisations of the nitrosyl anion $[Ir_6(CO)_{14}NO]^-$ can generate a disordered structure of C_{2v} symmetry, with the NO group statistically distributed over two different sites. This model rationalizes the solid-state structure of the $[N(PPh_3)_2]^+$ salt of $[Ir_6(CO)_{14}NO]^-$ (see Table 2) and is very similar to the molecular topology found for $[Ru_6C(CO)_{14}(NO)_2]$ [12], which possesses four truly bridging carbonyls.

Secondly, metallic skeletons can generate disordered packing structures if they are embedded within a highly symmetric ligand envelope. The very small charge separations on the molecular surface may not be sufficient to orient the molecule within the crystalline lattice. This is the case of the octahedral framework in the salt $[NEt_4][Ir_6(CO)_{14}NO]$ which was found to be disordered (in 60 : 40 ratio) about a pseudo-three-fold axis passing through two opposite faces of the metal octahedron, preventing resolution of the ligands. Therefore, we conclude that only subtle (and rather unpredictable) packing effects in the different crystals are responsible for the crystallization of the NO-containing carbonyl cluster with an *ordered* metal core and single orientation of the nitrosyl. Only after having prepared four different ammonium or phosphonium salts and having completed four structural determinations (reported in Table 2) we have found a crystal which allowed us confidently to infer the NO stereochemistry.

3. Experimental details

All the solvents were purified and dried by conventional methods and stored under dinitrogen. All the reactions were carried out under oxygen-free dinitrogen using the Schlenk-tube technique. $[N(PPh_3)_2]_2[Ir_6(CO)_{15}]$ was prepared by literature methods. [5,17] IR spectra were recorded on a Perkin-Elmer 16C FT-IR spectrophotometer using calcium fluoride cells previously purged with N_2. Elemental analyses were carried out at Laboratorio di Analisi of the Dipartimento di Chimica Inorganica, Metallorganica e Analitica.

3.1. Preparation of $[N(PPh_3)_2][Ir_6(CO)_{14}NO]$

$[N(PPh_3)_2]_2[Ir_6(CO)_{15}]$ (0.300 g; 0.113 mmol) and THF (15 ml) were placed in a Schlenk tube. When the cluster had dissolved, solid $(C_7H_7)[PF_6]$ (0.027 g; 0.113 mmol) was added and the completeness of the oxidation was checked by IR spectroscopy. The solution was cooled to −78°C with an acetone/dry ice bath, and NO bubbled through twice for about 15 s each time until the solution turned dark. The mixture was then warmed to room temperature and cyclohexane (20 ml) was added dropwise, inducing the precipitation of colourless $[N(PPh_3)_2\ [PF_6]$. This was filtered off and discarded. The solvent was removed in vacuum and the residue dissolved in MeOH. The crude product was precipitated by dropwise addition of water and collected by filtration. Crystals were grown by layering cyclohexane over a THF solution of the cluster. Anal. Calc.: for $C_{50}H_{30}Ir_6N_2O_{15}P_2$: C, 28.1; H, 1.3; N, 1.3. Found: C, 28.1; H, 1.6; N, 1.2%.

The salt $[NMe_3(CH_2Ph)][Ir_6(CO)_{14}NO]$ used for X-ray analysis was prepared using $[NMe_3(CH_2Ph)]_2[Ir_6(CO)_{15}]$ and crystals were grown from CH_2Cl_2/cyclohexane. Anal. Calc.: for $C_{24}H_{16}Ir_6N_2O_{15}$: C, 16.7; H, 0.9; N, 1.6. Found: C, 17.2; H, 1.2; N, 1.5%.

The salts of $[NEt_4]^+$ and $[PPh_4]^+$ were obtained similarly, and crystallized from CH_2Cl_2/cyclohexane.

3.2. Crystal structure determination of $[NMe_3(CH_2Ph)][Ir_6(CO)_{14}NO]$

A summary of crystal data collection and analysis parameters used in the structural determination is reported in Table 3. The diffraction experiments were performed on an Enraf-Nonius CAD4 diffractometer at room temperature, using graphite monochromatized Mo Kα radiation ($\lambda = 0.71073$ Å). The unit cell parameters and the orientation matrix were determined by least-squares fitting of the setting angles of 25 intense reflections in the $22° < 2\theta < 28°$ range. Monitoring of the diffracted intensities of three intense reflections showed a crystal decay of about 6% (on I) over the data collection period. The diffraction intensities were corrected for Lorentz polarization, decay, and absorption effects. This was achieved on the basis of ψ-scans ($\psi = 0$–360°, every 10°) of three suitable reflections having χ values near 90°. The structure was solved by direct methods (SIR92 [18]) and difference Fourier techniques, and refined by full-matrix least squares, the minimized function being $\Sigma w(F_0^2 - kF_c^2)^2$. Individual weights were assigned as $w = 1/[\sigma^2(F_0^2) + (0.0533P)^2 + 14.90P]$, where $P = (\max\ (0,F_0^2) + 2F_c^2)/3$. The iridium atoms were assigned anisotropic temperature factors. The anisotropisation of the carbonyl atoms, leading to an insignificant lowering of the agreement factors, resulted in two imaginary ellipsoids and was therefore rejected. The contribution of hydrogen atoms to the structure factors was neglected. The chirality of the crystal was tested by refining two enantiomeric models (in $P3_1$ and $P3_2$, respectively). Slightly better agreement factors and a reasonable Flack test [19] [0.02(4)] were found in $P3_1$, to which our final coordinates refer.

Table 3
Crystal data and data collection parameters for $[NMe_3(CH_2Ph)][Ir_6(CO)_{14}(NO)]$

Compound	$[NMe_3(CH_2Ph)][Ir_6(CO)_{14}NO]$
Formula	$C_{24}H_{16}Ir_6N_2O_{15}$
Formula weight, amu	1725.59
Crystal system	Trigonal
Space group	$P3_1$
a, Å	12.150(4)
c, Å	19.593(18)
V, Å^3	2505(3)
Z	3
D_{calc}, g cm^{-3}	3.432
T,°C	22(1)
λ, Å	0.71073
μ(Mo–Kα), cm^{-1}	238.8
$F(000)$	2268
Min. transm. factor	0.275
Scan mode	ω
Scan range	$3 < \theta < 25$
Scan width	$1.0 + 0.35\tan(\theta)$
No. Collected reflections	3253
Octants explored	$-h, k, l$
Crystal decay	6% on I
No. indep. reflections $I > 3\sigma(I)$	2135
No. variables	219
Refinement on	F^2
Weights	$1/[\sigma^2(F^2) + (0.0533P)^2 + 14.90P]$ [a]
R [b]	0.036
$wR2$ [b]	0.087
GOF [c]	1.078
Max. peak final diff. fourier, e Å^{-3}	1.6

P [a] $= [\max(0, F_o^2) + 2F_c^2]/3$.
R [b] $= \Sigma \| F_o |^2 - k | F_c |^2 | / \Sigma | F_o |^2$; $wR2 = [\Sigma w(| F_o |^2 - k | F_c |^2)^2 / \Sigma w F_o^2]^{1/2}$
GOF [c] $= [\Sigma w(| F_o |^2 - k | F_c |^2)^2 / (N_{obs} - N_{var})]^{1/2}$ where N_{obs} and N_{var} are the number of observations and refined parameters, respectively.

Table 4
Fractional atomic coordinates and equivalent isotropic displacement parameters (Å^2) for $[NMe_3(CH_2Ph)][Ir_6(CO)_{14}(NO)]$. U_{eq} is defined as one third of the trace of the orthogonalized U_{ij} tensor

Atom	x	y	z	U_{eq}
Ir(1)	0.16256(13)	0.27406(14)	0.00	0.0394(4)
Ir(2)	0.24864(13)	0.19135(12)	−0.10673(8)	0.0343(3)
Ir(3)	0.28483(13)	0.43532(13)	−0.10978(6)	0.0337(3)
Ir(4)	0.40356(13)	0.48824(14)	0.01340(7)	0.0341(3)
Ir(5)	0.3707(2)	0.24639(14)	0.01998(7)	0.0434(4)
Ir(6)	0.49285(13)	0.40372(13)	−0.09253(6)	0.0364(4)
O(1)	−0.038(4)	0.0324(3)	0.048(2)	0.108(11)
O(2)	−0.028(2)	0.045(2)	−0.0755(12)	0.058(6)
O(3)	0.146(3)	0.123(3)	0.122(2)	0.076(8)
O(4)	0.419(2)	0.707(2)	−0.0666(12)	0.063(7)
O(5)	0.266(3)	−0.046(3)	−0.1279(14)	0.073(8)
O(6)	0.161(3)	0.186(3)	−0.253(2)	0.089(9)
O(7)	0.367(3)	0.522(3)	−0.2537(14)	0.073(8)
O(8)	0.036(3)	0.432(3)	−0.1200(14)	0.072(7)
O(9)	0.671(3)	0.675(3)	0.061(2)	0.090(9)
O(10)	0.275(3)	0.536(3)	0.1336(14)	0.067(7)
O(11)	0.531(3)	0.348(3)	.0148(2)	0.081(9)
O(12)	0.379(4)	−0.002(4)	0.026(2)	0.111(11)
O(13)	0.501(3)	0.295(3)	−0.228(2)	0.101(10)
O(14)	0.683(3)	0.672(3)	−0.131(2)	0.089(9)
O(15)	0.685(5)	0.360(4)	−0.021(2)	0.16(2)
N(1)	0.045(3)	0.306(3)	0.0288(14)	0.052(7)
C(2)	0.077(3)	0.128(3)	−0.062(2)	0.038(7)
C(3)	0.189(3)	0.174(3)	0.071(2)	0.047(8)
C(4)	0.374(3)	0.593(3)	−0.056(2)	0.044(8)
C(5)	0.257(3)	0.044(3)	−0.1190(14)	0.033(7)
C(6)	0.198(3)	0.193(3)	−0.195(2)	0.053(9)
C(7)	0.336(3)	0.489(3)	−0.199(2)	0.039(7)
C(8)	0.129(3)	0.433(3)	−0.116(2)	0.041(7)
C(9)	0.569(3)	0.598(3)	0.044(2)	0.045(8)
C(10)	0.318(3)	0.513(3)	0.087(2)	0.040(7)
C(11)	0.473(4)	0.312(3)	0.099(2)	0.055(9)
C(12)	0.373(3)	0.096(3)	0.022(2)	0.044(8)
C(13)	0.485(3)	0.330(3)	−0.179(2)	0.041(7)
C(14)	0.613(3)	0.567(3)	−0.114(2)	0.052(9)
C(15)	0.587(4)	0.353(4)	−0.046(2)	0.082(13)
N(2)	0.962(3)	0.634(3)	0.206(2)	0.057(8)
C(16)	0.830(5)	0.610(5)	0.187(3)	0.09(2)
C(17)	0.974(5)	0.522(6)	0.185(3)	0.11(2)
C(18)	0.975(7)	0.657(7)	0.287(5)	0.15(3)
C(19)	1.064(3)	0.758(4)	0.172(2)	0.054(9)
C(20)	1.050(4)	0.743(4)	0.091(2)	0.071(11)
C(21)	1.130(4)	0.696(4)	0.060(2)	0.078(13)
C(22)	1.117(5)	0.689(5)	−0.015(3)	0.10(2)
C(23)	1.026(6)	0.709(6)	−0.043(3)	0.10(2)
C(24)	0.972(5)	0.777(5)	−0.022(3)	0.10(2)
C(25)	0.981(5)	0.791(5)	0.055(3)	0.09(2)

All the computations were performed on a Silicon Graphics Indigo computer running IRIX 4.01, using the SHELX93 suite of programs [20] and the physical constants tabulated therein. The final fractional atomic coordinates are listed in Table 4.

The supplementary material including full list of bond distances and angles, and a table of anisotropic thermal factors (Us) has been deposited with the Cambridge Crystallographic Data Center.

Acknowledgments

This work was supported by the Ministero della Università e della Ricerca Scientifica e Tecnologica and the Consiglio Nazionale delle Ricerche, Roma.

References and notes

[1] A. Cinquantini, P. Zanello, R. Della Pergola, L. Garlaschelli and S. Martinengo, *J. Organomet. Chem., 412* (1991) 215.

[2] (a) R. Della Pergola, L. Garlaschelli, S. Martinengo, F. Demartin, M. Manassero and N. Masciocchi *J. Chem. Soc., Dalton Trans.* (1988) 2307; (b) R. Della Pergola, L. Garlaschelli, S. Martinengo, F. Demartin, M. Manassero, N. Masciocchi, R. Bau and D. Zhao, *J. Organomet. Chem., 396* (1990) 385.

[3] A. Ceriotti, R. Della Pergola, F. Demartin, L. Garlaschelli, M. Manassero and N. Masciocchi, *Organometallics, 11* (1992) 756.

[4] R. Della Pergola, E. Brivio, L. Garlaschelli, N. Masciocchi and M. Manassero, *J. Cluster Sci., 5* (1994) 363.

[5] R.E. Stevens, P.C.C. Liu and W.L. Gladfelter, *J. Organomet. Chem., 287* (1985) 133.

[6] W.L. Gladfelter, *Adv. Organomet. Chem., 24* (1985) 41.

[7] R.E. Stevens, T.J. Yanta and W.L. Gladfelter, *Inorg. Synth., 22* (1983) 163.

[8] R.E. Stevens and W.L. Gladfelter, *Inorg. Chem., 22* (1983) 2034.

[9] ORTEP *A Fortran thermal-ellipsoid program for crystal structure illustration*, Johnson, C.K. Oak Ridge National Laboratory, Oak Ridge, TN, 1971.

[10] See for example: (a) V. Albano, P. Bellon, G. Ciani and M. Manassero, *J. Chem. Soc., Chem. Commun.* (1969) 1242; (b) R.J. Goudsmit, P.F. Jackson, B.F.G. Johnson, J. Lewis, W.J.H. Nelson, J. Puga, M.D. Vargas, D. Braga, K. Henrick, M. McPartlin and A. Sironi, *J. Chem. Soc., Dalton Trans.* (1985) 1795; (c) A. Gourdon and Y. Jeannin, *J. Organomet Chem., 440* (1992) 353; (d) B.F.G. Johnson, J. Lewis, W.J.H. Nelson, J. Puga, D. Braga, K. Henrick and M. McPartlin, *J. Organomet. Chem., 266* (1984) 173.

[11] See for example: (a) A.V. Rivera, G.M. Sheldrick, *Acta Crystallogr., B34* (1978) 3372; (b) D.E. Fjare and W.L. Gladfelter, *J. Am. Chem. Soc., 106* (1984) 4799; (c) J. Puga, R. Sanchez-Delgado and D. Braga, *Inorg. Chem., 24* (1985) 3971; (d) A. Gourdon and Y. Jeannin, *Organometallics, 5* (1986) 2406; (e) T. Chihara, K. Sawamura, H. Ogawa and Y. Wakatsuki, *J. Chem. Soc., Chem. Commun.* (1994) 1179; (f) A. Gourdon and Y. Jeannin, *J. Organomet. Chem., 282* (1985) C39.

[12] B.F.G. Johnson, J. Lewis, W.J.H. Nelson, J. Puga, P.R. Raithby, D. Braga, M. McPartlin and W. Clegg, *J. Organomet. Chem., 243* (1983), C13.

[13] K. Henrick, B.F.G. Johnson, J. Lewis, J. Mace, M. McPartlin and J. Morris, *J. Chem. Soc., Chem. Commun.*, (1985), 1617.

[14] The Q value measures the maximum deviation of the M–M edges from their average value; it was defined in R. Della Pergola, L. Garlaschelli, S. Martinengo, F. Demartin, M. Manassero, N. Masciocchi, R. Bau and D. Zhao, *J. Organomet. Chem., 396* (1990), 385.

[15] R. Della Pergola, F. Demartin, L. Garlaschelli, M. Manassero, S. Martinengo, N. Masciocchi and M. Sansoni, *Organometallics, 10* (1991) 2239, and references therein.

[16] D. Braga and F. Grepioni, *J. Organomet. Chem., 336* (1987), C9.

[17] M. Angoletta, L. Malatesta and G. Caglio, *J. Organomet. Chem., 94* (1975) 99.

[18] A. Altomare, G. Cascarano, C. Giacovazzo, A. Guagliardi, M.C. Burla, G. Polidori and M. Camalli, *J. Appl. Crystallogr., 27* (1994) 435.

[19] H.D. Flack, *Acta Cryst., A39* (1983), 876; G. Berardinelli and H.D. Flack, *Acta Cryst., A41* (1985) 500.

[20] G.M. Sheldrick, SHELX93, *J. Appl. Cryst.*, (1994) in press.